

# Secretagogue-induced calcium wave shows higher and prolonged transients of nuclear calcium concentration in mast cells

Satoshi Katagiri, Tetsuro Takamatsu\*, Tetsuhiro Minamikawa, Setsuya Fujita

*Department of Pathology, Kyoto Prefectural University of Medicine, Kawaramachi Hirokoji, Kamigyo-ku, Kyoto 602, Japan*

Received 20 September 1993

To clarify the mechanism of secretagogue (compound 48/80)-induced calcium signaling in rat peritoneal mast cells, we analyzed serial confocal calcium images with high spatial and temporal resolution using different  $\text{Ca}^{2+}$ -probes. The  $\text{Ca}^{2+}$ -wave began at the periphery of the cytoplasm, and then spread to the center of the nucleus. Nuclear  $[\text{Ca}^{2+}]_i$  was clearly higher than cytoplasmic  $[\text{Ca}^{2+}]_i$ . The heterogeneity of  $[\text{Ca}^{2+}]_i$  continued until about 2 min after degranulation. These results suggest the existence of an intranuclear  $\text{Ca}^{2+}$ -store which possesses a  $\text{Ca}^{2+}$ -releasing mechanism similar to that in the cytoplasm.

Mast cell; Calcium ion concentration; Confocal laser scanning microscopy; Exocytosis; Nucleus; Compound 48/80

## 1. INTRODUCTION

The spatiotemporal changes of calcium signals in the form of waves, which may have important roles in the regulation of various biological processes, have been observed in many cell types [1–4]. Although elevation of cytosolic  $[\text{Ca}^{2+}]_i$  following the production of inositol 1,4,5-trisphosphate ( $\text{IP}_3$ ) has been reported in mast cell exocytosis [5], the spatiotemporal distribution of  $[\text{Ca}^{2+}]_i$  as signaling for degranulation has not yet been studied in detail. To understand the mechanism regulating exocytosis, it is important to understand how calcium signals spread within a single mast cell.

Compound 48/80 is a secretagogue, inducing a rapid increase of cytoplasmic  $[\text{Ca}^{2+}]_i$  in rat mast cells and subsequent histamine release [6]. It is well known that both IgE-mediated and compound 48/80-induced exocytosis are accompanied by phosphoinositide breakdown [7].

In the present study, the spatial and temporal profiles of  $\text{IP}_3$ -mediated calcium signals in mast cells were analyzed using a confocal laser scanning microscope and a calcium-sensitive indicator, fluo-3 [8] or indo-1 [9]. Confocal fluorescence images revealed compound 48/80 evoked  $[\text{Ca}^{2+}]_i$  wave propagation at average speeds of  $35 \mu\text{m/s}$  through the cytoplasm and the nucleus. It is remarkable that the high nuclear  $[\text{Ca}^{2+}]_i$  was maintained for about 2 min after degranulation. Ratioed measurements of  $[\text{Ca}^{2+}]_i$  with fura-2 [9] revealed that the peak nuclear  $[\text{Ca}^{2+}]_i$  was over  $1.2 \mu\text{M}$ , much higher than the cytoplasmic  $[\text{Ca}^{2+}]_i$  of around  $1.0 \mu\text{M}$ . Our data suggests the presence of calcium stores in the nucleus en-

abling the calcium wave to propagate at a constant speed almost equal to that in the cytoplasm and  $\text{Ca}^{2+}$  permeability barriers in the nuclear membrane to prevent the diffusion of  $[\text{Ca}^{2+}]_i$  from nucleus to cytoplasm.

## 2. MATERIALS AND METHODS

### 2.1. Cell preparation

Male Wistar rats weighing 200–300 g were ether-anesthetized and exsanguinated by carotid section. Peritoneal cells including mast cells were obtained by washing the peritoneal cavity with 20 ml of modified Ringer's solution, comprising 150 mM NaCl, 2.8 mM KCl, 2 mM  $\text{CaCl}_2$ , 1 mM  $\text{MgCl}_2$ , 10 mM glucose, 1 mg/ml bovine serum albumin, and 10 mM HEPES–NaOH, pH 7.3 [10]. Collected cells were washed twice with Ringer's solution by centrifugation  $150 \times g$  for 5 min each time.

### 2.2. Loading procedures

The cell suspension was loaded with an acetoxymethyl ester (AM) form of fluorescence calcium indicator fluo-3 ( $20 \mu\text{M}$ ; Dojindo, Japan) for 1 h at room temperature in Ringer's solution containing 10% fetal calf serum in 0.06% pluronic F-127 (BASF, USA) [11] and placed onto an experimental chamber on the stage of a microscope. In some experiments, the suspension was loaded with fura-2/AM or Indo-1/AM ( $5 \mu\text{M}$ , Dojindo) for 30 min at room temperature in the same solution as above. To analyze the influence of extracellular  $\text{Ca}^{2+}$  on intracellular  $\text{Ca}^{2+}$  signaling, the chamber was perfused in some experiments with  $\text{Ca}^{2+}$ -free solution (150 mM NaCl, 2.8 mM KCl, 1 mM  $\text{MgCl}_2$ , 2 mM EGTA, 10 mM glucose, 10 mM HEPES–NaOH, pH 7.3), instead of Ringer's solution.

Compound 48/80 (final concentration;  $10 \mu\text{g/ml}$ ) was added to the bathing solution (Ringer's solution). In local application, the secretagogue was applied directly onto the cell by means of pressure ejection from a micropipette filled with 1 mg/ml of compound 48/80.

### 2.3. Confocal microscopy

The system for confocal observation of living cells has been fully described previously [12]. In the present study, the equipment consisted of a laser scanning microscope (Olympus LSM-GI), an image processor (Imaging Technology Inc, Series 150/151, USA), and a host

\*Corresponding author. Fax: (81) (75) 251-5353.

computer (Sanyo MBC-18TJ, Japan). The argon laser beam (wavelength 488 nm, 10 mW) was focused with an objective lens (Olympus SPlan-Apo, 60  $\times$ : NA 1.4, oil-immersion). Fluorescent light was led to a photomultiplier through a dichroic mirror (500 nm) and a pinhole aperture (50  $\mu$ m) to create a confocal image. After digitizing through an 8-bit A/D converter, fluorescence intensity data was stored in a 512  $\times$  512  $\times$  8-bit frame memory in the image analyzer for image storage and processing.

Our ultraviolet confocal laser scanning microscopy (UV-CLSM) system [13] consisted of an UV argon ion laser (Coherent, Enterprise 622, USA; 351+364 nm, >50 mW), an inverted Olympus IMT-2 microscope with a confocal laser scanning unit (Olympus GI200UV), the image processor, and the host computer. The UV argon ion laser beam was focused with a water-immersion objective lens (Olympus UV ApoLSM 100  $\times$ : NA 1.1). For indo-1 excitation, the peak ultraviolet emission at a wavelength of 351 nm was used selectively by employing a short-pass filter (355 nm). Indo-1 fluorescence was split with a dichroic mirror (450 nm), and that at two different wavelengths was simultaneously measured through interference filters (405 nm and 480 nm; bandwidth, both 20 nm) with photomultipliers.

Scan modes employed in the present study are shown in Fig. 1.

#### 2.4. Detection of the nucleus

Some preparations were doubly stained with fluo-3 and the DNA-specific fluorochrome, 4',6-diamidino-2-phenylindole (DAPI). Preparations were first stained with 5  $\mu$ g/ml DAPI in Ringer's solution for 6 h at 37°C and then loaded with fluo-3/AM (20  $\mu$ M) for 1 h. Confocal fluorescence images of the nucleus with DAPI were obtained by UV-CLSM.

#### 2.5. $[Ca^{2+}]_i$ measurements with fura-2

$[Ca^{2+}]_i$  was measured with fura-2, the dual excitation indicator. Cells were loaded as described in Loading procedures. Fluorescence images of a fura-2-loaded single mast cell were obtained with an objective lens (Zeiss Plan-Neofluar, 100  $\times$ : NA 1.30, oil-immersion) mounted on an inverted microscope (Zeiss Axiovert 35) through a CCD camera (Hamamatsu Photonics, C2400-77, Japan). Fluorescence images were obtained at excitation wavelengths of 340 and 380 nm with an emission wavelength of 510 nm. The ratioing of images ( $R_{340/380}$ ) was achieved by image processor dividing of the 340 nm image by the 380 nm image on a pixel-by-pixel basis.  $[Ca^{2+}]_i$  for individual cells was calculated through calibration with fura-2-containing EGTA- $Ca^{2+}$  buffers [9].

### 3. RESULTS

#### 3.1. Confocal X-Y scan images

Fig. 2 shows consecutive X-Y scan fluo-3-images of  $[Ca^{2+}]_i$  after stimulation of compound 48/80 in a single mast cell. Individual images were created by X-Y-scanning with 80 ms intervals from top to bottom.  $[Ca^{2+}]_i$  elevation began at the periphery of the cell and subsequently proceeded toward the center. Nuclear  $[Ca^{2+}]_i$  was clearly higher than cytoplasmic  $[Ca^{2+}]_i$ . The confocal images stained with DAPI and fluo-3 revealed that the part of the cell with higher  $[Ca^{2+}]_i$  after stimulation exactly coincided with the nucleus (Fig. 3). This heterogeneity of  $[Ca^{2+}]_i$  in a single cell continued until 2 min after degranulation (data not shown). The confocal image with indo-1 showed that, prior to stimulation, nuclear  $[Ca^{2+}]_i$  was a little lower than cytoplasmic  $[Ca^{2+}]_i$ , but after stimulation nuclear  $[Ca^{2+}]_i$  was obviously higher than that in the cytoplasm (Fig. 4).

#### 3.2. Confocal X-t scan images

Using the rapid X-t scanning mode (2 ms/line), com-

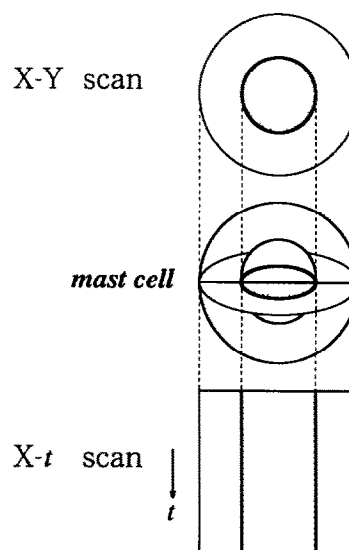


Fig. 1. X-Y and X-t scan modes. X-t scan mode provided a time-plotted fluorescence image along a single horizontal line across the cell with high temporal resolution.

pound 48/80-induced elevation and propagation of  $[Ca^{2+}]_i$  in a single mast cell was observed in the standard (Ringer's) external solution (Fig. 5). The transient increase in  $[Ca^{2+}]_i$  began at the periphery of the cytoplasm, and spread to the center of the cell to the nucleus. Degranulation was detected 10–20 s after the calcium wave was observed. Calcium wave propagation also occurred in  $Ca^{2+}$ -free solution (data not shown).

When compound 48/80 was locally applied through a micropipette (Fig. 6), the  $[Ca^{2+}]_i$  wave began at the site of stimulation and spread to the other side of the cell through the nucleus at a constant speed (Fig. 7). Degranulation was initiated close to the site of stimulation. The average speed of travel across the cell was 35  $\mu$ m/s, ranging from 32–42  $\mu$ m/s after both local and whole cell application of compound 48/80.

#### 3.3. Quantitative fura-2 fluorescence imaging

To estimate absolute values of cytosolic and nuclear  $[Ca^{2+}]_i$  after stimulation, we employed a ratiometric method with the dual excitation indicator fura-2. Fig. 8 shows the calibrated  $[Ca^{2+}]_i$  image after stimulation with compound 48/80 in a single mast cell. The nuclear  $[Ca^{2+}]_i$  was estimated at over 1.2  $\mu$ M, whereas that in the cytoplasm reached a maximum of nearly 1  $\mu$ M.

### 4. DISCUSSION

#### 4.1. Calcium wave and exocytosis

We demonstrated spatial and temporal changes of secretagogue (compound 48/80)-induced calcium signaling in mast cells. Images detected by CLSM (Figs. 4,5) revealed that secretagogue-induced calcium signaling travels at a constant speed (average 35  $\mu$ m/s) through the whole cell, from the periphery of the cell to the center of the nucleus. These observations indicate

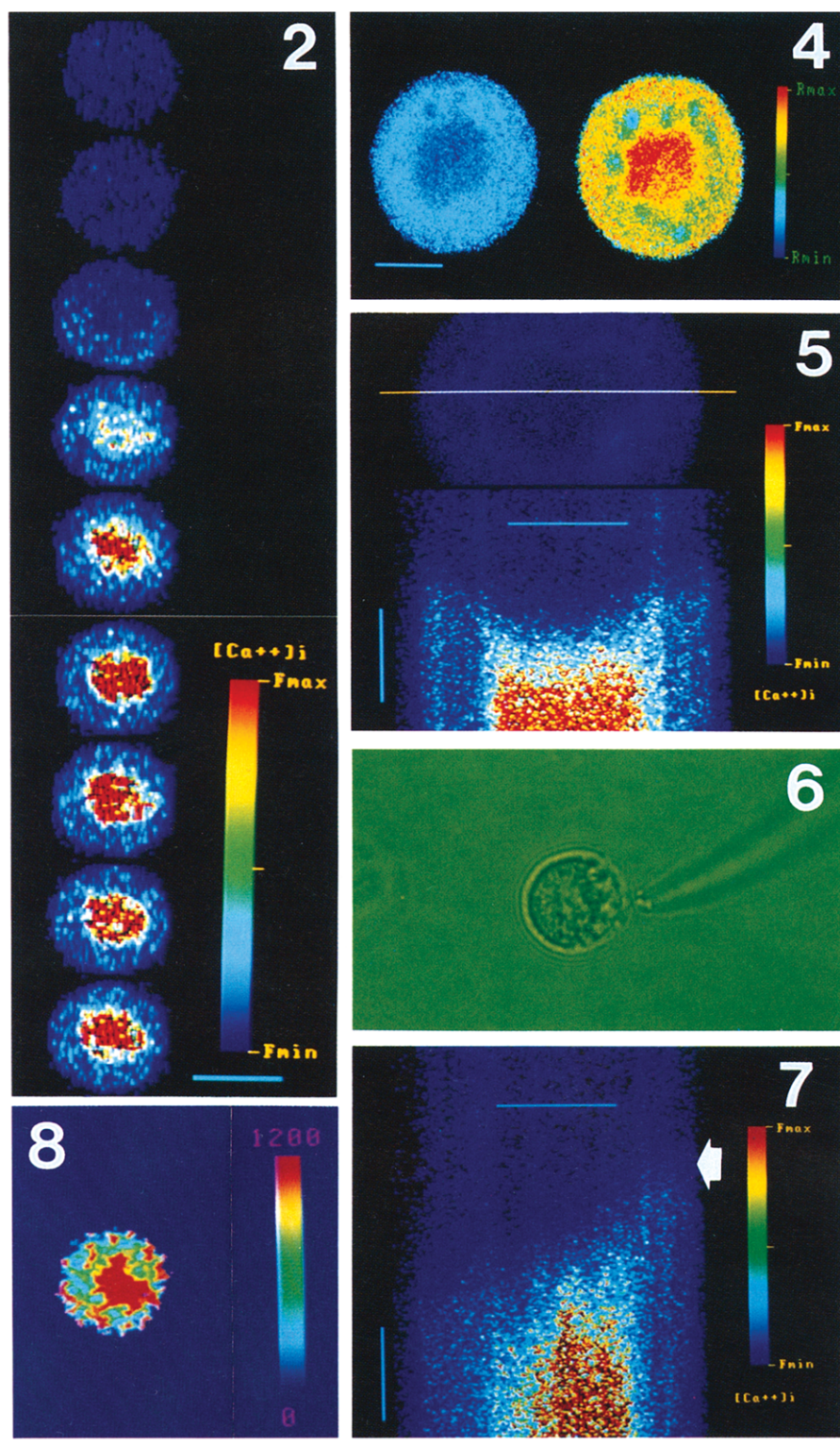


Fig. 2. *X-Y* scan images of calcium wave propagation induced by bath application of the secretagogue. Consecutive confocal images at intervals of 80 ms after compound 48/80 stimulation showing the elevation of cytoplasmic  $[Ca^{2+}]_i$  in the third image and elevation of nuclear  $[Ca^{2+}]_n$  in the fourth image.  $[Ca^{2+}]_n$  in the nucleus was apparently higher than that in the cytoplasm. The blue horizontal bar represents 10  $\mu m$ .

Fig. 4. *X-Y* scan images of the indo-1-loaded mast cell before (left) and after (right) compound 48/80 stimulation (10  $\mu g/ml$ ). Right image was obtained immediately after the degranulation. Nuclear  $[Ca^{2+}]_n$  was higher than cytoplasmic  $[Ca^{2+}]_i$ . The blue horizontal bar represents 5  $\mu m$ .

Fig. 5. *X-t* scan imaging of calcium wave propagation induced by bath application of the secretagogue. The mast cell was repeatedly scanned along the white horizontal line indicated in the top image at 2 ms/scanning line.  $[Ca^{2+}]_i$  wave initially rose at the peripheral region of the cytoplasm and spread to the center of the cell including the nucleus. The blue bar represents 200 ms vertically and 5  $\mu m$  horizontally.

Fig. 6. Local application of the secretagogue through a micropipette. The secretagogue was applied directly onto the cell by means of pressure ejection from the micropipette.

Fig. 7. *X-t* scan imaging of calcium wave propagation induced by local application of the secretagogue.  $[Ca^{2+}]_i$  wave proceeded from the side closest to the micropipette (arrow) across the cell to the other side. The blue bar represents 200 ms vertically and 5  $\mu m$  horizontally.

Fig. 8. Image of fura-2 fluorescence in a single mast cell after compound 48/80 stimulation (10  $\mu g/ml$ ). The image was obtained immediately after degranulation. Nuclear  $[Ca^{2+}]_n$  (over 1.2  $\mu M$ ) was obviously higher than cytoplasmic  $[Ca^{2+}]_i$  (about 1.0  $\mu M$ ).

that calcium signaling in mast cells can propagate in the nucleus as well as in the cytoplasm. It has been reported that stimulation with antigen or compound 48/80 evokes the first calcium signal depending on  $IP_3$ -induced calcium release from internal calcium stores [14,15], and that subsequent propagation is driven by a

sequence of calcium diffusion and amplification steps, and calcium-induced calcium release from intracellular stores [16].

Our confocal *X-t* scan images showed that immediately after touching the edge of the nucleus, the calcium wave, with the speed unchanged, suddenly showed



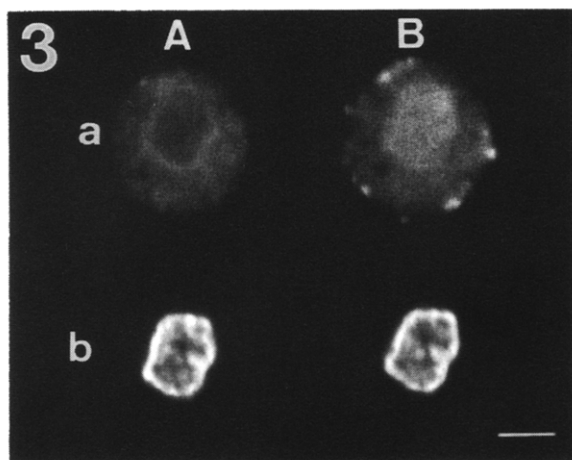


Fig. 3. X-Y scan images of a mast cell co-loaded with fluo-3 and DAPI before (A) and after (B) compound 48/80 stimulation (10  $\mu\text{g}/\text{ml}$ ). (a) fluo-3, (b) DAPI image. Images after stimulation were obtained immediately after degranulation. The region of higher fluo-3 fluorescence intensity geometrically matched the nuclear region stained with DAPI. The horizontal bar represents 5  $\mu\text{m}$ .

higher  $[\text{Ca}^{2+}]_i$  and passed through the nucleus with that high concentration. Although the existence of a calcium store in the nucleus has yet to be determined, several authors have recently reported the presence of ATP- and calmodulin-dependent  $\text{Ca}^{2+}$  uptake or  $\text{IP}_3$ -sensitive  $\text{Ca}^{2+}$  release mechanisms near or within the nucleus [17–19]. In mast cells there may be calcium stores in the nucleus that can release  $\text{Ca}^{2+}$  in response to high  $[\text{Ca}^{2+}]_i$  with speeds equal to those observed in the endoplasmic reticulum.

#### 4.2. Nuclear $[\text{Ca}^{2+}]_i$

Nuclear  $[\text{Ca}^{2+}]_i$  was clearly higher than cytoplasmic  $[\text{Ca}^{2+}]_i$ , and was not an artifact of calcium indicators as heterogeneity of  $[\text{Ca}^{2+}]_i$  in fluo-3 images after stimulation of mast cells was confirmed in the present study by two different  $\text{Ca}^{2+}$  probes, i.e. fura-2 or indo-1 fluorescence images (Figs. 4, 8). It is postulated that the nuclear membrane possesses a barrier mechanism to prevent diffusion of  $[\text{Ca}^{2+}]_i$  from nucleus to cytoplasm and to sustain high nuclear  $[\text{Ca}^{2+}]_i$  for a few minutes after degranulation. Similar heterogeneity of  $[\text{Ca}^{2+}]_i$  between nuclear  $[\text{Ca}^{2+}]_i$  and cytoplasmic  $[\text{Ca}^{2+}]_i$  has been reported in several cell types such as B lymphoma cells (BAL17 cells) [20], cultured smooth muscle cells (DDT<sub>1</sub>MF<sub>2</sub> cells) [21], basophilic leukemia cells (RBL-

2H3 cells) [22] and cultured neurons [23]. However, the nature of this barrier remains unknown.

Sustained high nuclear  $[\text{Ca}^{2+}]_i$  may play an important role in the regulation of nuclear events such as activation of nuclear enzymes [24, 25] that may, in the degranulation of mast cells, associate with newly synthesized, lipid-derived mediators or post-degranulation recovery processes.

#### REFERENCES

- [1] Gilkey, J.C., Jaffe, L.F., Ridgway, E.B. and Reynolds, G.T. (1978) *J. Cell Biol.* 76, 448–466.
- [2] Takamatsu, T. and Wier, W.G. (1990) *FASEB J.* 4, 1519–1525.
- [3] Takamatsu, T. and Wier, W.G. (1990) *Cell Calcium* 11, 111–120.
- [4] Kasai, H. and Augustine, G.J. (1990) *Nature* 348, 735–738.
- [5] Penner, R., Matthews, G. and Neher, E. (1988) *Nature* 334, 499–504.
- [6] White, J.R., Ishizaka, T., Ishizaka, K. and Sha'afi, R.I. (1984) *Proc. Natl. Acad. Sci. USA* 81, 3978–3982.
- [7] Cockcroft, S. and Gomperts, B.D. (1979) *Biochem. J.* 178, 681–687.
- [8] Kao, J.P., Harooturian, A.T. and Tsien, R.Y. (1989) *J. Biol. Chem.* 264, 8179–8184.
- [9] Grynkiewicz, G., Poenie, M. and Tsien, R.Y. (1985) *J. Biol. Chem.* 260, 3440–3450.
- [10] Kuno, M., Okada, T. and Shibata, T. (1989) *Am. J. Physiol.* 256, C560–C568.
- [11] Poenie, M., Alderton, J., Steinhardt, R. and Tsien, R. (1986) *Science* 233, 886–889.
- [12] Takamatsu, T., Minamikawa, T., Kawachi, H. and Fujita, S. (1991) *Cell Struct. Funct.* 16, 341–346.
- [13] Minamikawa, T., Takamatsu, T., Kashima, S., Fushiki, S., Fujita, S. (1993) *Micron* 24 (in press).
- [14] Neher, E. and Almers, W. (1986) *EMBO J.* 5, 51–53.
- [15] Hoth, M. and Penner, R. (1992) *Nature* 355, 353–356.
- [16] Berridge, M.J. (1991) *Cell Calcium* 12, 63–72.
- [17] Burgoyne, R.D., Cheek, T.R., Morgan, A., O'Sullivan, A.J., Moreton, R.B., Berridge, M.J., Mata, A.M., Colyer, J., Lee, A.G. and East, J.M. (1989) *Nature* 342, 72–74.
- [18] Nicotera, P., McConkey, D.J., Jones, D.P. and Orrenius, S. (1989) *Proc. Natl. Acad. Sci. USA* 86, 453–457.
- [19] Malviya, A.N., Rogue, P. and Vincendon, G. (1990) *Proc. Natl. Acad. Sci. USA* 87, 9270–9274.
- [20] Yamada, H., Mizuguchi, J., Nakanishi, M. (1991) *FEBS Lett.* 284, 249–251.
- [21] Himpens, B., De Smedt, H., Droogmans, G. and Casteels, R. (1992) *Am. J. Physiol.* 263, C95–C105.
- [22] Nakato, K., Furuno, T., Inagaki, K., Teshima, R., Terano, T. and Nakanishi, M. (1992) *Eur. J. Biochem.* 209, 745–749.
- [23] Birch, B.D., Eng, D.L. and Kocsis, J.D. (1992) *Proc. Natl. Acad. Sci. USA* 89, 7978–7982.
- [24] Masmoudi, A., Labourdette, G., Mersel, M., Huang, F.L., Huang, K.-P., Vincendon, G. and Malviya, A.N. (1989) *J. Biol. Chem.* 264, 1172–1179.
- [25] Divccha, N., Rhee, S.G., Letcher, A.J. and Irvine, R.F. (1993) *Biochem. J.* 289, 617–620.